Journal of Pharmaceutical Innovation
https://doi.org/10.1007/s12247-023-09752-3

ORIGINAL ARTICLE

# Novel Nanoaggregates from *Phoenix dactylifera* (date palm) for Inhalational Management of Cystic Fibrosis Using Dry Powder Inhalers

**Hadeel Aburass[1] · Nisreen Dahshan[1] · Hamad Alyami[2] · Affiong Iyire[3] · Eman Zmaily Dahmash[4]**

Accepted: 23 June 2023


## Abstract

**Purpose** *Phoenixdactylifera* extracts have shown efficacy as antioxidants and antibacterials for the treatment of lung diseases; however, the choice of route of administration remains a problem. The use of natural antibacterial remedies for the management of cystic fibrosis (CF) is promising due to recurring bacterial resistance to current antibiotics. Dry powder inhalers (DPIs) have also been identified as a patient-friendly, noninvasive method for local delivery of drugs to the lungs. Therefore, this work, which is the first of its kind, aimed to formulate nanoparticles of date palm extracts as DPIs and evaluate their aerodynamic and antibacterial biofilm characteristics for the potential treatment of CF.

**Method** Chitosan-based nanoparticles (CDN) comprising aqueous date fruit extract with increasing concentrations of chitosan (0.05, 0.1, and 0.2% w/v) were prepared. The in vitro aerosolization of the formulations was studied using a next-generation impactor (NGI), and good aerosolization profiles were achieved. The produced nanoparticles were characterized using FTIR and XRD to confirm physical properties and TEM and zeta sizer to confirm shape and size. The antimicrobial activity of CDN was evaluated using a *Pseudomonas aeruginosa* biofilm model cultured in an artificial sputum medium (ASM) mimicking cystic fibrosis conditions in the lungs.

**Results** Nanoparticles containing 0.05% w/v chitosan demonstrated the highest encapsulation efficiency (55.91%) and delivered the highest emitted dose (98.92%) and fine particle fraction (42.62%). CDN demonstrated the first-time-ever reported significant 3.3 log-cycle inhibition of *P. aeruginosa* biofilm cultured in ASM. TEM images revealed the formation of spherical particles with an average size of $42.98 \pm 19.19$ nm. FTIR and XRD studies demonstrated the compatibility of the components with the presence of the characteristic features of chitosan and date powder.

**Conclusions** This novel work showcases CDN as a prophylactic adjuvant for the management of cystic fibrosis using DPI.

**Keywords** Cystic fibrosis · Date palm · Dry powder inhaler · Nanoparticles · *Phoenix dactylifera* · *Pseudomonas aeruginosa* biofilm

## Abbreviations

| | |
|---|---|
| ASM | Artificial sputum medium |
| CDN | Chitosan-based nanoparticles |
| CFTR | Cystic fibrosis transmembrane conductance regulator |
| CFU | Colony-forming unit |
| CS | Cystic fibrosis |
| DPIs | Dry powder inhalers |
| ED | Emitted dose |
| EE | Encapsulation efficiency |
| FPF | Fine particle fraction |
| FPF-ED | Fine particle fraction of emitted dose |
| FPF-ND | Fine particle fraction of nominal dose |
| GSD | Geometric standard deviation |
| LOX | Lysyl oxidase |
| MBC | Minimum bactericidal concentration |
| MIC | Minimum inhibitory concentration |
| MMAD | Mass median aerodynamic diameter |
| NF-kB | Nuclear factor kappa B |

✉ Eman Zmaily Dahmash
e.dahmash@kingston.ac.uk

[1] Department of Applied Pharmaceutical Sciences, Faculty of Pharmacy, Isra University, Amman 11622, Jordan

[2] Department of Pharmaceutics, College of Pharmacy, Najran University, Najran 55461, Saudi Arabia

[3] Aston Pharmacy School, Aston University, Birmingham B4 7ET, UK

[4] Department of Chemical and Pharmaceutical Sciences, School of Life Sciences, Pharmacy and Chemistry, Kingston University London, Kingston upon Thames KT1 2EE, UK

Published online: 14 July 2023

| | |
|---|---|
| NGI | New-generation impactor |
| OD600 | Optical density |
| RD | Respirable dose |
| SD | Standard deviation |

## Introduction

The prevalence of cystic fibrosis (CF) is 1 in 2500, with the carrier frequency of CF as 1 in 28 in North American white populations and 1 in 84 in African Americans [1]. CF is an inherited disorder due to a mutation of the cystic fibrosis transmembrane conductance regulator (CFTR) gene that causes severe damage to the lungs, digestive system, and reproductive organs. The CFTR gene is responsible for the regulation of chloride ion transport across the cell membrane. Defects in this gene cause unnatural movement of salt and water across cells and affect the cells that produce mucus, sweat, and digestive juices, resulting in the production of sticky and thick secretions that block passageways, ducts, and tubes, especially in the lungs and pancreas [2]. There is no known cure for CF, and the most common complications come from lung infections. Acute lung infections are treated with antibiotics, which may be given intravenously, by inhalation, or by mouth [3]. Excessive thick mucus will lead to blockage of distal airways, which limits pathogen clearance and host defense causing recurrent infections by providing a favorable environment for bacterial growth. *Pseudomonas aeruginosa* is the main pathogen leading to lung infection in CF patients. Chronic infection of *Pseudomonas aeruginosa* in CF patients is associated with biofilm formation. The formation of biofilm highly increases antibiotic resistance, leading to ineffective treatments [4]. Managing CF entails using airway clearance therapies, anti-inflammatory medications, and antibiotics for treatment and prophylaxis. Oral, intravenous (IV), and aerosolized antibiotic formulations are indicated for use in CF patients [3]. However, as the resistance of *Pseudomonas aeruginosa* to many antibiotics is emerging, the need for alternative management options is high.

Long-term use of antibiotics can improve clinical status, improve lung function, and improve survival. However, it causes adverse effects such as diarrhea, skin rashes, candidiasis, ototoxicity, and nephrotoxicity and leads to the emergence of antibiotic resistance [5]. Despite ongoing efforts for developing new antibiotics, the use of antibiotic adjuvants is prevailing as an alternative approach to overcome bacterial resistance. These adjuvants have the potential to be used alone or in combination with commonly used antibiotics to reduce resistance, reduce the dose, or broaden the spectrum of antibiotic activity. Such strategies prolong the life span of available antibiotics [6, 7].

Date fruits (*Phoenix dactylifera* L.) contain carbohydrates, salts, minerals, dietary fibers, vitamins, fatty acids, and amino acids [8]. Ferulic, p-coumaric, flavonoids, sinapic acids, and procyanidins contribute to the antioxidant activity of date fruit [9–12]. Research findings indicated that date fruit consists of 13 flavonoid glycosides of quercetin, apigenin, and luteolin. Constituents of dates such as flavonoids and phenolics have an important role in cancer control via the regulation of key genetic pathways that demonstrated no side effects [13]. Recently, Badawi [14] investigated the antioxidant and antibacterial properties of nanoparticles prepared from date seeds and reported approximately 100-fold and 1.2-fold increases, respectively, in the antioxidant and antibacterial properties of the nanoparticles compared with the date seed extracts. The transcription factors LOX and NF-kB play a critical role in cancer, diabetes, inflammation, infection, and other diseases. Regulation of these factors is a significant process in the prevention of different diseases. Flavonoids and phenols, which are constituents of date fruit, act as anti-inflammatory and antibacterial agents [15]. Furthermore, previous studies have reported the efficacy of date sap for the treatment of lung injuries. After application to a murine model of pulmonary fibrosis, results demonstrated that date sap can attenuate bleomycin-induced lung fibrosis due to its richness in phenolic compounds, vitamins, anti-oxidative, and anti-fibrotic effects [16, 17]. Dry powder inhalers (DPIs) are an ideal delivery choice to reduce adverse effects since they act locally by delivering antibiotics or other drugs directly to the lungs and reaching infected airways, therefore allowing effective treatment of lung infections. In addition to that, DPIs enhance patient adherence to the medication [5]. Therefore, the aim of this study was to develop nanoparticles made from date fruit extract with chitosan polymer using an ionotropic gelation technique, deliver these to the lungs using a dry powder inhaler, and assess the antimicrobial activity against *Pseudomonas aeruginosa* as a potential antibiotic adjuvant for the management of CF. The produced nanoparticles were further characterized for their physical properties using X-ray diffraction (XRD), Fourier transform infrared (FTIR), transmission electron microscopy (TEM), and zeta sizer.

## Materials and Methods

### Materials

Zahidi date powder was donated by Woods pur Farms (CA, USA). Magnesium citrate (CAS 7779-25-1) was purchased from Sinopharm Chemical Reagent Co. Ltd., (Mainland, China). Glycerin (CAS 56-81-5), glycine (CAS 56-40-6), and L-cysteine (CAS 52-90-4) were obtained

from Guangdong Guanghua Chemical Factory Co. Ltd. (Guangdong, China). DNA from fish sperm (CAS 100403-24-5), cellulase (CAS 9012-54-8), chitosan (low molecular weight (LMW)) (CAS 9012-76-4), and mucin from the porcine stomach (type II) (CAS 84082-64-4) were purchased from Sigma Aldrich (Steinheim, Germany). Essential amino acids (L-histidine (CAS 71-00-1), L-isoleucine (CAS 73-32-5), L-leucine (CAS 61-90-5), L-lysine (CAS 56-87-1), L-methionine (CAS 63-68-3), L-phenylalanine (CAS 63-91-2), L-threonine (CAS 72–19-5), L-tryptophan (CAS 73–22-3), and L-valine (CAS 72-18-4), as well as nonessential amino acids (L-alanine (CAS 56-41-7), L-arginine (CAS 74-79-3), L-asparagine (CAS 70-47-3), L-aspartic acid (CAS 56-84-8), L-cysteine (CAS 52-90-4), L-glutamine (CAS 56-85-9), L-glycine (CAS 56-40-6), L-proline (CAS 147-85-3), L-serine (CAS 56-45-1), and L-tyrosine (CAS 60-18-4)), were purchased from Sigma Aldrich (USA). Tris (hydroxymethyl) aminomethane (CAS 77-86-1) and diethylenetriamine penta-acetic acid (CAS 67-43-6) were purchased from SD Fine-Chem Limited (Mumbai, India). Potassium hydroxide (KOH) (CAS 1310-58-3), potassium chloride (KCl) (CAS 7447-40-7), and sodium chloride (NaCl) (CAS 7440-23-5) were obtained from AZ Chemicals, Inc. (ON, Canada). Egg yolk emulsion, nutrient agar, and nutrient broth were purchased from Biolab (Budapest, Hungary). Hard gelatin capsules size 3 were donated from Pharmacare (Amman, Jordan). Acetic acid (CAS 64-19-7) was purchased from Labchem (NJ, USA) and acetone (CAS 67-64-1) was obtained from Alpha Chemika (India).

## Preparation of Chitosan Date Extract Nanoparticles

Chitosan-based nanoparticles (CDN) were prepared using the method described by Badawi [14] with modifications. The ionotropic gelation technique was employed to produce nanoaggregates as an alternative to the carrier-based formulation for the delivery of dry powder inhaler formulation. This technique is optimum for the encapsulation of extracts, using chitosan nanoparticles to encapsulate the date fruit extract [14]. Initially, chitosan polymer was dissolved in acetic acid to produce various concentrations (0.2 g (F1), 0.1 g (F2), and 0.05 g (F3) in 50 mL of 1% (v/v) acetic acid). The viscosity of these solutions was determined for 10 min using an Ubbelohde glass capillary viscometer Rheotek, Poulten Selfe & Lee Ltd. (Essex, England) with the temperature set at 20 °C. The chitosan solution was then placed on a magnetic stirrer at 100 rpm for 24 h at room temperature. After that, the pH was adjusted to 5 using 1 N NaOH. The date fruit extract was prepared by weighing 10 g of the date fruit powder and marinating it in 100 mL of distilled water for 48–72 h at room temperature. After adding the chitosan solution dropwise, 50 mL of the filtered extract with 120 mg of the cross-linker, sodium chloride. The solution was kept at room temperature for 24 h with continuous stirring at 110 rpm. Next, the solution was centrifuged using a Hettich Universal 30 RF centrifuge device (Germany) at a speed of 11,000 rpm for 30 min, with the removal of any residual acetic acid. The precipitate was placed in the oven at 30 °C to dry for 24 h. Upon drying, the powder was ground using a mortar and pestle, and then the powder was sieved using a sieve with an aperture size of 32 µm. The powder was kept in an airtight container until required.

## Physicochemical Characterization

### Hydrodynamic Particle Size Analysis

The mean hydrodynamic particle size, polydispersity index (PDA), and zeta potential of chitosan powder, palm date fruit powder, and the produced CDN were determined using the Malvern Zetasizer Nano ZS90 (Malvern Instrument, UK). A small quantity (~5 mg) of each sample was suspended in 10 mL of distilled water and a bath sonicated for 30 s to break agglomerates. The temperature was set to 25 °C, and each sample was measured in triplicate.

### Fourier Transform Infrared Spectroscopy

FTIR spectra of date powder, chitosan, and CDN samples were recorded using a Perkin Elmer FTIR spectrometer (OH, USA). The Spectrum 10 software was employed for the analysis of the produced spectra. Prior to measurement, a few milligrams of the sample were placed on the laser lens. For each sample, the FTIR spectral scans were recorded to cover a range of 500–4000 $cm^{-1}$ with a resolution of 2 $cm^{-1}$.

### Transmission Electron Microscopy

To enhance understanding of the morphological composition of the nanoparticles, the CDN sample was analyzed using a transmission electron microscope (JEOL-JEM-2100F, Japan) and a high-resolution TEM (HR-TEM) attached with selected area electron diffraction. A small amount of powder was suspended in water, and TEM analyses were acquired by adding almost 5 µL of the CDN suspension onto a copper grid and drying for 10 h at room temperature. The experiments were run at an accelerating voltage of 200 kV without any further modification or coating of the sample. The ImageJ software (Fiji) version 1.53t was used to calculate the particle size of the produced nanoparticles.

### X-ray Diffraction

XRD analysis for the CDN was conducted using an X-ray diffractometer model D8 Phaser from Bruker AXS (Germany). The processing conditions were as follows: X-ray generator set at 30 kV and 10 mA using Co tube with LYNXEYE detector. The diffractions were recorded over a ($2\theta$) range from 4 to 50° at a rate of 0.02° $2\theta$ $s^{-1}$. The Topas software (Bruker, AXS) was employed to generate and analyze the produced diffraction peaks.

### Encapsulation Efficiency

To calculate the encapsulation efficiency (EE) of CDN, the following procedure was used. Firstly, the mixture containing the CDN was centrifuged at 11,000 rpm for 30 min. The supernatant was separated from the pellets at the end of the centrifugation. Secondly, the amount of the free compounds in the supernatant was measured based on measuring the absorbance by UV-spectrophotometry at lambda max 350 nm. The encapsulation efficiency of date powder was calculated according to Eq. (1).

$$\mathrm{EE}\% = \frac{\text{Total amount of date extract} - \text{Total amount of free date extract}}{\text{Total amount of date extract}} \times 100 \quad (1)$$

### Assessment of Aerodynamic Performance of the CDN Using the New-Generation Impactor

The developed formulation was filled into size 3 hard gelatin capsules and tested using a new-generation impactor (NGI; Copley Scientific Limited, Nottingham, UK). For each run, 6 capsules of 20 mg each were used. The Aerolizer® was used as the actuation device. Trays of NGI were treated with 1% glycerin in an acetone solution and left to dry. The purpose of conditioning is to prevent particles from bouncing back. Tray weights were measured before and after each actuation. The formulations were run at a flow rate of 60 ± 5 L/min to produce a pressure drop of 4 kPa. The pre-separator was filled with 15 mL of distilled water. Each actuation was run over 4 s. Results were used to assess the aerodynamic parameters such as fine particle fraction (FPF), respirable dose (RD), emitted dose (ED), and mass median aerodynamic diameter (MMAD). RD was defined as the total mass of the particles that settled on the NGI trays from trays 2 to 7. The mass of the particle was measured by weighing each tray before and after performing the NGI. The calculations were based on 6 capsules per batch, and each capsule contained 20 mg of the CDN—fit the aerosolized. The FPF of the emitted dose (FPF-ED) was calculated by dividing the RD by the emitted dose, whereas the FPF of the nominal dose (FPF-ND) was calculated based on the RD divided by the theoretical (nominal) dose. The emitted dose was calculated based on the cumulative content obtained from the induction tube, pre-separator, and trays 1 to 8. The calculations of MMAD were according to the USP method < 601 > [18]. Using a flow rate of 60 L/min, the MMAD was calculated based on previous work [19]. All results were generated in triplicates and reported as mean ± SD.

## Biological Characterization

### Assessment of Biological Activity of CDN and Date Fruit Extract

For the assessment of the biological activity, the minimum inhibitory concentration (MIC) and minimum bactericidal activity of the CDN and ethanolic date extracts were tested. The effect of *Pseudomonas aeruginosa* biofilm cultured in an artificial sputum medium (ASM) that resembles cystic fibrosis sputum was evaluated. ASM was prepared following the method by Kirchner et al. [20] (Table 1). For the preparation of date fruit extract, 10 g of date powder was soaked in 100 mL of ethanol for 48 h at room temperature, then the extract was centrifuged at 11,000 rpm for 20 min (Hettich Universal 30 RF, Germany) and filtered to obtain a clear solution. The solution was placed to dry in a water bath at 50 °C until the ethanol was completely evaporated. The residue was stored at − 20 °C in an amber-colored bottle until use.

### MIC and MBC Test for CDN and Date Fruit Extract

Overnight culture of *Pseudomonas aeruginosa* (ATCC 15692) in nutrient agar plates at 37 °C was adjusted in nutrient broth to match 0.5 McFarland. Solutions of CDN and 100% ethanolic date extract are first diluted to the proper concentration using nutrient broth, and then serial half dilutions of 100 µL are made in 96-well plates using nutrient broth. The concentrations of 100% ethanolic extract from 366 to 15 mg/mL and concentrations of CDN from 18 to 0.75 mg/mL were tested. The bacterial suspension was added to each well in 10 µL volumes (*ca.* 1.5 × 106 CFU). The MIC was considered the lowest concentration with no visible *Pseudomonas aeruginosa* growth or turbidity, and the minimum biocidal concentration was considered the lowest concentration with no growth. Each test was repeated three times.

**Table 1** Summary of materials and processing conditions for the development of ASM

| Ser no. | Material/process | Quantity | Medium/volume | Conditions |
|---|---|---|---|---|
| 1. | Fresh sperm DNA | 4 g | Sterile water/250 mL | Dissolved slowly for 24 h at room temperature (solution 1) |
| 2. | Porcine stomach mucin (type II) | 5 g | Sterile water/250 mL | Dissolved slowly at room temperature (solution 2) |
| 3. | All amino acids (excluding L-tyrosine and L-cysteine) | 250 mg from each amino acid | Sterile water/100 mL | Dissolved slowly at room temperature (solution 3) |
| 4. | L-cysteine | 250 mg | 0.5 M KOH/25 mL | Dissolved slowly at room temperature (solution 4) |
| 5. | L-tyrosine | 250 mg | Sterile water/25 mL | Dissolved slowly at room temperature (solution 5) |
| 6. | Diethylenetriaminepentaacetic acid (DTPA), NaCl, and KCl | 5.9 mg/5 g/2.2 g | Sterile water/100 mL | Dissolved slowly at room temperature (solution 6) |
| 7. | Combine solutions 1–6 into 1 L bottle then add egg yolk emulsion | 5 mL | Add sterile water to make a total of 850 mL | Mix at room temperature |
| 8. | pH adjustment | Quantity sufficient from the buffer | 1 M Tris buffer (pH 8.5) | Adjust to pH 6.9 |
| 9. | Adjust total solution volume | Up to 1 L | Sterile water | |
| 10. | Filtration sterilization | | | Syringe filter 0.20 µm |
| 11. | Storage at 4 °C in the dark | | | Stable for 4 weeks |

### Biofilm Formation

Biofilm culture on ASM was prepared according to the procedure described by Kirchner et al. [20]. The day before the experiment, *Pseudomonas aeruginosa* was cultured in nutrient agar plates and incubated overnight at 37 °C. Eighty milligrams of either CDN (F3) or date ethanolic extract was added to 6 mL of sterile ASM to obtain a final concentration of 13 mg/mL in each solution (solutions A and B). Furthermore, 12 mg of chitosan powder was added to 6 mL of sterile ASM to produce 2 mg/mL of chitosan solution (solution C). Moreover, an additional ASM alone was considered a control (solution D). In a 24-well plate, 1.8 mL of each solution (A, B, C, and D) was added to three wells (3 replicates each). The overnight culture of *Pseudomonas aeruginosa* was diluted in nutrient broth to an optical density ($OD_{600}$) of $0.1 \pm 0.02$ Au/cm. The ASM (solutions A, B, C, and D) was inoculated with 18 µL of the bacterial suspension in all wells, while the negative control contained ASM only. Finally, the 24-well plate was secured with laboratory parafilm and incubated in a shaker incubator for 48 h at 37 °C while shaking at 75 rpm (Lab Shaker Incubator model: IN-666 (Gemmyco Taipei, Taiwan)). After incubation, 100 µL of 100 mg/mL cellulase (diluted in 0.05 M citrate buffer) was added to all wells to disrupt the bacterial biofilms, and the plate was incubated at 37 °C for 1 h while shaking at 150 rpm. Manual pipetting of the biofilms was then done to ensure disruption. The ASM-containing wells were serially diluted, and 100 µL of each dilution was cultured on nutrient agar plates and incubated overnight at 37 °C. Colonies were counted from the plates to determine the CFU/mL. Log-transformed bacterial counts (CFU/mL) were evaluated.

### Statistical Analysis

All experiments carried out in replicates were reported as mean ± standard deviation (SD). Where needed, one-way or two-way ANOVA as well as Tukey post-test were reported using Minitab v. 18 statistical pack. The level of significance was set at 0.05. For NGI experiments, 6 capsules were used from each batch.

## Results and Discussion

### Physicochemical Characterization of Formulated CDN

Three formulations were prepared, and the produced CDN resulted in a fine and fluffy powder. Chitosan is a polymer that requires an acidic environment to dissolve; therefore, a 1% v/v acetic acid solution was used. Acetic acid is the most widely used solvent, and its concentration depends on the molecular weight of chitosan [21]—LMW chitosan was used. Acidic solutions result in the protonation of the amine group of chitosan and hence increase solubility [22]. However, the acidic solvent type alters the properties of the polymer [23]. Studies showed that using acetic acid solvent reduced the water vapor uptake when compared to lactic acid-based solvents, which is favorable for inhalation

formulations [23, 24]. Also, reports demonstrated that chitosan-based materials using acetic acid produced formulations with higher rigidity, antibacterial activity, and a lower tendency to deform in comparison with samples prepared using lactic acid solvent [23].

### FTIR and XRD Analysis

FTIR spectra of chitosan powder as can be seen from Fig. 1a showed all characteristic bands for polysaccharides. A strong band around 3300 $cm^{-1}$ corresponds to N–H stretching, O–H stretching, and the intramolecular hydrogen bonds. Whereas the absorption bands at around 2866 $cm^{-1}$ are attributed to C–H stretching [25]. The troughs at 1645 $cm^{-1}$ and 1315 $cm^{-1}$ indicate the presence of *N*-acetyl groups (stretching of the C = O and C–N of the amide group, respectively). Additional characteristic troughs at 1120 $cm^{-1}$ can be attributed to the asymmetric stretching of the C–O–C, while two additional bands at 1064 and 1026 $cm^{-1}$ correspond to C–O stretching. The results of this work are in concordance with other reported results [26–28].

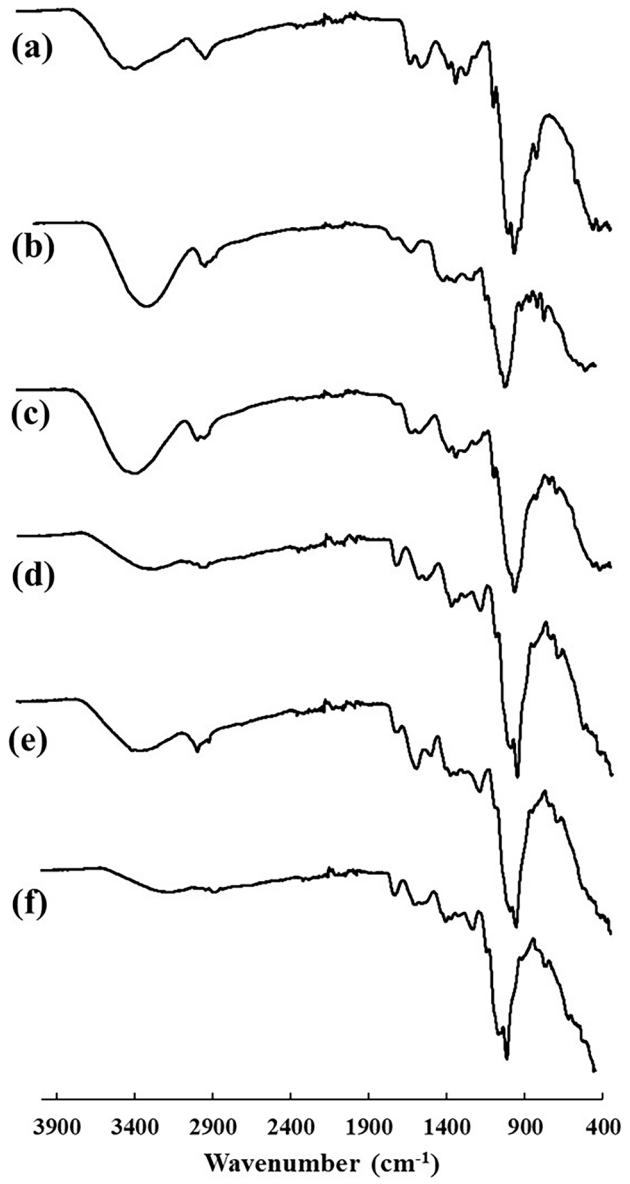


**Fig. 1** FTIR spectra of (**a**) chitosan powder, (**b**) date palm fruit powder, (**c**) chitosan:date fruit powder physical mixture, (**d**) F1, **e** (F2), and (**f**) F3 over the wavenumber range from 450 to 4000 $cm^{-1}$

FTIR analysis of crude palm date fruit powder showed troughs and peaks that represent either stretching, bending, or vibration of specific bonds. Figure 1b depicts a wide trough at around 3306 $cm^{-1}$, which is assigned to hydroxyl group O–H stretching. This has been reported to correspond to cellulose and water content [29]. The characteristic trough noted at 2913 $cm^{-1}$ was attributed to C–H stretching vibrations, whereas troughs at 1612 and 1015 $cm^{-1}$ were assigned to carbonyl (C = O) and C–OH stretching, respectively. Such results tally with results obtained from Farhadi and colleagues [30]. The FTIR spectra of the physical mix of chitosan and date fruit powders can be seen in Fig. 1c. Apparently, there is an overlap between bands; however, some characteristic bands for either chitosan and or date fruit could be seen in the physical blend. Furthermore, the FTIR spectra of the CDN formulations F1, F2, and F3 (Fig. 1d–f) demonstrated a similar pattern to that of the date powder, with a slight reduction in the trough within the range of 2900 $cm^{-1}$. The change is related to the percentage of chitosan used and the amount of entrapped date fruit extract. Overall, no change in date composition upon inclusion in the CDN was observed.

X-ray diffraction studies of date palm fruit powder (Fig. 2a) demonstrated the crystalline nature of its content, owing to the sharp peaks at $2\theta = 11.78°$, 13.2°, 18.92°, 19.42°, 22.14°, 24.86°, 31.06°, and 32.02°. This is the first report of XRD for date powder or extracts in the literature. XRD of chitosan powder (Fig. 2b) demonstrated the amorphous nature of chitosan with a wide peak at $2\theta = 20°$ and a sharp peak at 20°, which is in line with the reported results in the literature [31–34]. The physical mixture of chitosan and date fruit powder, as can be seen in Fig. 2c, showed the characteristic diffraction of dates fruit powder and chitosan. Furthermore, chitosan containing date fruit extract for the three formulations can be seen in Fig. 2d–f. The three XRD patterns showed similar trends with broad peaks at $2\theta = 10°$ and $2\theta = 20°$, related to chitosan [31]. However, lower chitosan concentrations as in F2 and F3 showed a sharp peak at around $2\theta$ of 26° and could represent the crystalline component of date extract. In conclusion, as expected, the CDN retained the key characteristic features of chitosan material.

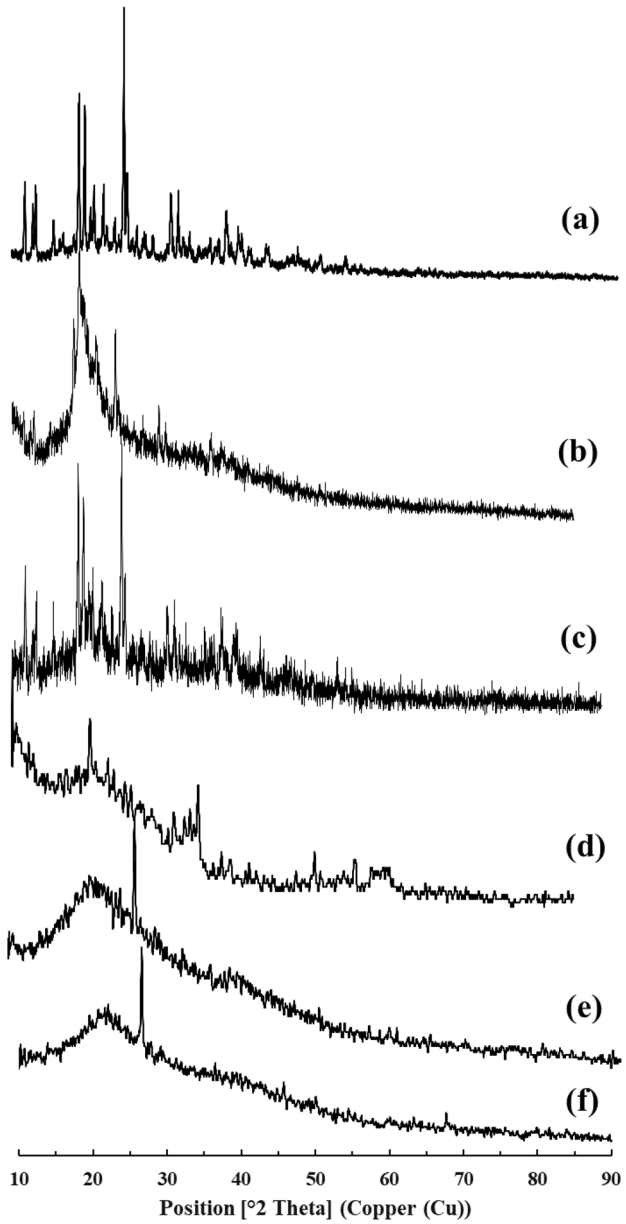


**Fig. 2** XRD pattern of the (**a**) date palm fruit powder, (**b**) chitosan powder, (**c**) chitosan:palm fruit powder physical mix, (**d**) F1, (**e**) F2, and (**f**) F3

### Particle Size and Surface Properties

Particle size and surface charge (zeta potential) analyses using the zeta sizer (Table 2) showed that raw materials (chitosan, palm date fruit powder, and the physical mix of both) presented as aggregated powders with large mean hydrodynamic particle size exceeding 1.15 µm, 1.01 µm, and 0.921 µm, respectively. The presence of aggregates and uneven size distribution was due to the high PDI for the three samples. However, the CDN nanoparticles exhibited a nanosize range between 98 and 156 nm, which is within the optimal range for drug delivery [35]. The average diameter of CDN was slightly higher (one-way ANOVA, $p = 0.148$) in formulations with higher chitosan content (F1: 0.2%), which agrees with other findings [36, 37]. Furthermore, the zeta potential values were measured for all the samples, and the chitosan particles displayed a positive value (+ 15.87 mV) that is attributed to the positively charged-$NH_3^+$ functional groups on chitosan's molecular chain [38]. Additionally, date palm fruit powder displayed a negative charge, which is thought to be due to the presence of negatively charged functional groups within the material. The addition of date fruit extract to chitosan during the entrapment process caused a reduction in the particles' negative charge, which could be attributed to the presence of the positively and negatively charged particles of chitosan and date fruit extract, respectively. The change of zeta potential was significant among CDN formulations (one-way ANOVA, $p = 0.000$), which is related to the amount of chitosan and the entrapment efficiency of the final formulation.

The next step was to assess the EE of the nanoparticles as an indication of their carrier efficiency, and thus, their ability to deliver higher doses to the respiratory system (see Table 3). The EE increased with a reduction in chitosan concentration. F1 with a chitosan concentration of 0.05% w/v, produced the highest entrapment efficiency of 55.91% ($p = 0.000$). Several researchers reported an increase in entrapment efficiency upon the reduction of chitosan concentration [39, 40]. This could be attributed to the lower viscosity of the medium of F3 (4.52 cP), which is associated

**Table 2** Particle size analysis (particle size, polydispersity index (PDI), and zeta potential) of chitosan powder, date palm fruit powder, physical mix, and the CDN (F1, F2, and F3) (mean ± SD, $n = 3$)

| Material | Particle size (nm) Mean ± SD, $n = 3$ | PDI Mean ± SD, $n = 3$ | Zeta potential (mV) Mean ± SD, $n = 3$ |
|---|---|---|---|
| **Chitosan powder** | 1150.25 ± 98.77 | 0.838 ± 0.054 | 15.87 ± 0.713 |
| **Date palm fruit powder** | 1005.55 ± 453.03 | 0.711 ± 0.212 | − 18.07 ± 0.819 |
| **Chitosan:date powder physical mix** | 921.25 ± 210.95 | 0.665 ± 0.076 | − 14.058 ± 0.423 |
| **F1** | 156.18 ± 32.95 | 0.341 ± 0.101 | − 3.093 ± 0.211 |
| **F2** | 135.66 ± 39.88 | 0.295 ± 0.174 | − 6.227 ± 0.389 |
| **F3** | 98.76 ± 18.21 | 0.305 ± 0.099 | − 10.357 ± 0.305 |

**Table 3** Viscosity and encapsulation efficiency (EE) of CDN using various concentrations of chitosan (mean ± SD, $n = 3$)

| Sample no. | Chitosan% (w/v) | Viscosity (cP) | EE% | $p$ value |
|---|---|---|---|---|
| F1 | 0.2 | 21.78 ± 4.57 | 21.66 ± 1.04 | 0.000 |
| F2 | 0.1 | 10.05 ± 3.99 | 46.01 ± 1.23 | |
| F3 | 0.05 | 4.52 ± 0.54 | 55.91 ± 0.70 | |

with a low chitosan concentration. This might enable a reduction in liquid phase resistance against dispersion and the formation of nanoparticles. Several studies also reported the effect of chitosan solution viscosity on entrapment efficiency [41, 42]. The change in encapsulation was most profound at higher chitosan concentrations. Similar results were reported by Vandenberg et al. [42].

## In Vitro Evaluation of the Aerodynamic Properties of the CDN Using NGI

Date fruit has many pharmacological properties, including antioxidant, anti-inflammatory, and antimicrobial properties. In general, the quantity of drug that is delivered to the targeted site of action is fundamental in the biological response and pharmacodynamic effect. Therefore, CDN should reach the lower parts of the lungs to produce the expected action. Therefore, this part of the study aimed at determining the efficiency of the formulation employing FPF, which is the most commonly used parameter to assess the in vitro aerodynamic properties of the formulations. The targeted FPF was more than 20%, and the desired ED was more than 60% in all formulations. Such targets were based on average results reported for marketed dry powder inhalers [43].

Figure 3 highlights the key aerodynamic parameters, namely, %ED, %FPF of the ED (%FPF-ED), RD, and %FPF of the nominated dose (FPF-ND). The results revealed that the CDN generated FPF-ED ranging from 21.50 to 42.56%, which exceeded the targeted range for the three formulations. From Fig. 3, F3 demonstrated significantly higher values of FPF-ND, FPF-ED, and RD (one-way ANOVA, $p < 0.05$). The results suggest that lower chitosan content resulted in less dense particles and hence better aerodynamic performance.

"The percentage of the nominal dose that is emitted from the dosage unit (capsule) upon actuation is expressed as the ED" [44]. From Fig. 3, there was no significant difference in ED among formulation (F1–F3) (94.5, 80.41, and 98.91, respectively) (one-way ANOVA, $p = 0.098$). Nevertheless, it was noted that F3 showed the lowest variation between runs as can be seen from the low magnitude of the error bars. Such results were expected as the light and fluffy produced from the three batches would support the pulmonary delivery of the formulations.

The second parameter was FPF-ED, which represents "the percentage of the emitted dose that can deposit into the lower region of the respiratory system (mainly alveoli) and has an aerodynamic particle size that ranges between 1 and 5 μm" [45, 46]. F3 had the highest FPF-ED of 42.56%, and the difference among formulations was statistically significant (one-way ANOVA, $p = 0.042$). In general, larger FPF may result in higher systemic availability of CDN [47]. Moreover, the results of FPF-ND had a good representation of the amount within the nominated dose that is deposited into the lower part of the lungs. FPF-ND in the three formulations showed a significant difference among formulations (one-way ANOVA, $p = 0.040$). All three formulations produced FPF-ND above the anticipated target of 20%; however, F3 was superior at 42.6%.

Figure 3 also presents the RD for the three formulations. F3 showed the highest RD (6.75 mg) per actuation followed by F2 (4.01 mg) and F1 (3.62 mg) per actuation. This

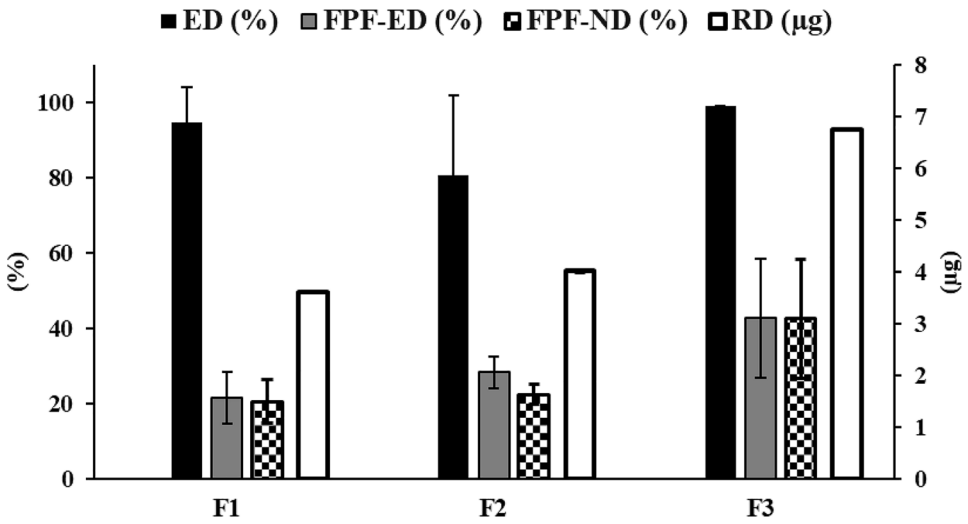


**Fig. 3** Summary of the in vitro aerodynamic performance of CDN using NGI. Each capsule contained 20 mg of the CDN. F1: 0.2% w/v chitosan, F2: 0.1% w/v chitosan, F3: 0.05% w/v chitosan. Results are presented as mean ± SD, $n = 3$. ED, %Emitted dose; FPF-ED, fine particle fraction from emitted dose; FPF-ND, fine particle fraction from nominated dose; RD, respirable dose

**Table 4** MMAD and GSD of the three CDN formulations

| Formulation | MMAD (μm) | GSD |
|---|---|---|
| **F1** | 1.46 ± 0.09 | 0.073 ± 0.01 |
| **F2** | 1.39 ± 0.11 | 0.070 ± 0.009 |
| **F3** | 1.31 ± 0.13 | 0.068 ± 0.011 |

difference was significant (one-way ANOVA, $p = 0.040$). The reduction in RD is attributed to the lower chitosan concentration resulting in less dense particles and hence enhanced deposition of the nanoparticles at the lower parts of the lungs. Previous research reported that the concentration of the chitosan solution plays a crucial role in affecting the particle size [37].

The MMAD results for F1–F3 are shown in Table 4. The MMAD results for CDN showed a statistically significant variation among formulations (one-way ANOVA, $p = 0.000$), ranging from 1.31 to 1.46 μm. The reduction of chitosan concentration resulted in lower particle size, and such results are in line with the aerodynamic parameters of the three formulations. Lower chitosan concentrations resulted in higher EE, ED, FPF, and RD. Furthermore, an examination of the geometric standard deviation (GSD) indicated that the three formulations produced particles with similar particle size distribution (GSD) (one-way ANOVA, $p = 0.427$). These results exhibited a potential strategy to deliver date fruit powder extract to the lower parts of the respiratory system. The CDN produced after freeze-drying generated nanoaggregates within the favorable aerodynamic particle size range of 1–5 μm. Once the aggregates are deposited into the alveoli region within the respiratory system, they tend to disperse into their primary nanosized particles, which will delay the fast clearance process and therefore have the potential for extended local effect [48].

Figure 4 illustrates the detailed distribution of particles through every stage in the NGI for F1–F3. It is divided into three sections; the first represents the extrathoracic deposition. This part involves particles that are larger than 8 μm, which will deposit into the upper parts of the respiratory system. The second part is pulmonary, which produces optimal pulmonary deposition (cutoff size of 1–5 μm). The third section represents the extrapulmonary (smaller particles that will not enter the respiratory system) and extrathoracic with particles exceeding 8 μm (particles deposited at the mouthpiece, induction tube, and stage 1). From the graph, F3 showed the lowest extrathoracic deposition while having the highest percentage of pulmonary deposition. Interestingly, the three formulations had limited extrapulmonary deposition. Furthermore, Fig. 5 shows the deposition of CDN in the stages of the NGI device. As can be noted from the graph (Fig. 4), deposition was mainly concentrated on trays 2–5.

The development of nanoaggregates is a key approach in pulmonary drug delivery. The aerodynamic performance of the developed CDN revealed the ability of the particles to produce micronized aerodynamic particles that can deposit on the lower parts of the respiratory system. The developed particles (formulation F3) were further assessed using TEM. Figure 6A, B highlights the agglomerated particles with an almost spherical shape. A closer look at the particles, as can be seen in Fig. 6C, D, reveals smooth surfaces with pores. Porous material supports the aerodynamic performance of the particles and, hence, effective pulmonary drug delivery. A study by Gharse and Fiegel [49] reported the enhanced aerodynamic properties of porous materials, which enable even larger particles to deposit deeper into the lung due to their low density when compared with less porous materials [49]. The particle size of the produced nanoparticles was measured using the ImageJ software (Fig. S1), which demonstrated an average particle size of 42.98 ± 19.19 nm ($n = 42$). However, it was noted that the exact particle diameter of the CDN as calculated from the TEM images using the ImageJ software was lower than the hydrodynamic diameter that was obtained using the zeta sizer for F3.

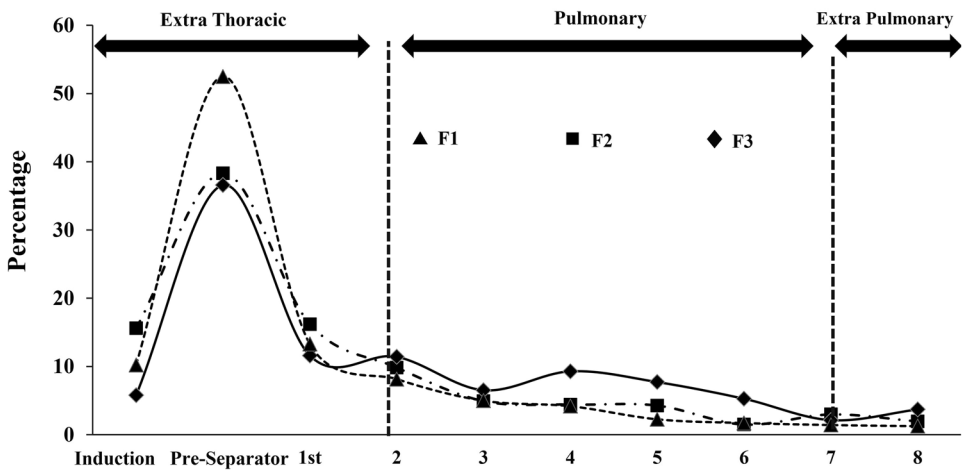


**Fig. 4** In vitro comparison of the aerodynamic particle size distribution of the three formulations demonstrating the lung deposition of CDN using NGI set at a flow rate of 60 L/min

**Fig. 5** Deposition of the chitosan date nanoparticles onto the NGI apparatus highlights the brown powder from trays 1 to 7 (labeled from left to right)

This discrepancy has been previously reported by various research findings, as the diffraction laser technique estimates the average diameter of the particles, including the hydration layer that surrounds the particles' outer surface, while the TEM image shows the exact diameter of the produced NPs [35, 50]. Furthermore, this difference also could

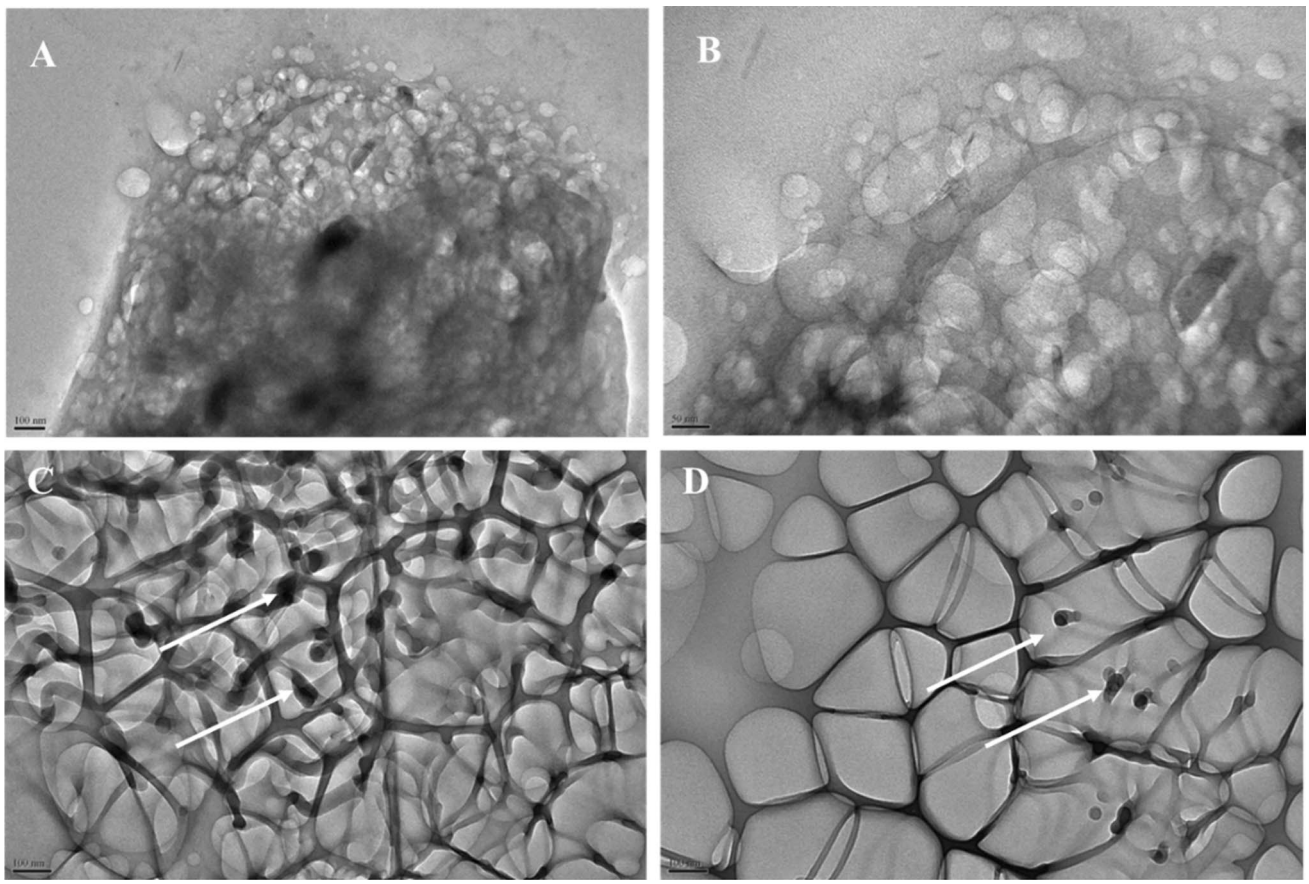


**Fig. 6** Morphological characterization of CDN (F3) using TEM. Arrows highlight the pores within the surface of the particles (with increasing magnifications **A**, **B**, **C**, and **D**, respectively)

be attributed to the formation of aggregates in the nanosuspension that increased the mean size.

## Biological Characterization

### Assessment of the Biological Activity of CDN and Extract

The next set of investigations focused on assessing the biological activity of the produced CDN. As discussed earlier, *Pseudomonas aeruginosa* is the main bacterium in cystic fibrosis. Hence, this part of the work assessed the antibacterial activity of CDN formulations using the *Pseudomonas aeruginosa* biofilm model cultured in ASM that mimics conditions in cystic fibrosis. Furthermore, the ethanolic extract was prepared and assessed to identify if different extracts showed antibacterial effects as well.

### MIC and MBC of Ethanolic Date Extract and CDN

MIC and MBC results showed the superior effect of CDN in comparison to 100% ethanolic extract (Table 5). Such results are in accordance with reports on the superiority of nanoparticles [30].

## Evaluation of Biofilm Inhibition

The activity of CDN against *Pseudomonas aeruginosa* biofilm, which is more resistant than the planktonic form, was evaluated. The thick mucus in the lungs of cystic fibrosis patients is a suitable condition for bacterial growth. Moreover, evaluation of the activity in conditions resembling CF mucus is of vital importance as the phenotypic characteristics of *P. aeruginosa* biofilm are related to nutritional conditions [4]. Date extract activity against *P. aeruginosa* has been previously reported [51, 52]. However, no inhibitory activity against *P. aeruginosa* biofilm grown in ASM-mimicking conditions in CF lungs has been assessed before. Therefore, this part of the work focused on assessing the ability of CDN and date ethanolic extract to inhibit biofilm formation in a model mimicking condition in CF by utilizing ASM as a culture medium for biofilm formation.

Date fruit ethanolic extract failed to inhibit biofilm formation (Fig. 7). Chitosan showed biofilm inhibitory activity for almost one log cycle. Whereas CDN resulted in a significant 3-log cycle reduction of the bacterial load. Knowing that cystic fibrosis patients will certainly have biofilms [3], this formulation could be introduced as a prophylactic treatment to prevent biofilm formation in CF patients or used as an antibiotic adjuvant in the management of CF.

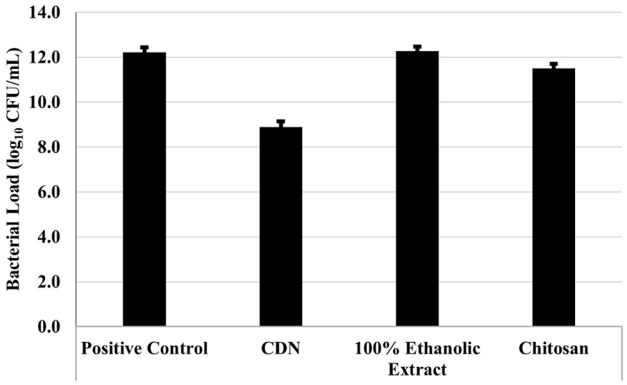


**Fig. 7** The effect of CDN (13.3 mg/mL) and the ethanolic date extract (13.3 mg/mL) and chitosan (2 mg/mL) on *Pseudomonas aeruginosa* biofilm grown in ASM after 48 h (mean ± SD, $n = 3$)

Several studies reported the antibacterial effect of date fruit extracts against other organisms such as *Escherichia coli*, *Staphylococcus aureus*, *Streptococcus pyogenes*, and *Pseudomonas aeruginosa* [53–55]. Furthermore, AlFaris [12] reported the powerful antioxidant activity of date fruit extract due to the presence of phenolic compounds. The anti-inflammatory, antioxidant, and antibacterial activities of palm date fruit extract were also reported in several publications [11, 30, 55–57]. This provides the potential for investigating the effect of a developed CDN on other respiratory conditions.

Following the interesting results from formulated CDN, future studies need to investigate the release pattern of the produced nanoparticles and conduct in vivo studies to evaluate the effectiveness of such formulations; along with the scalability and cost-effectiveness of the approach. Further research could explore the long-term safety and efficacy of the treatment, as well as potential side effects and patient adherence to inhalation therapy.

**Table 5** MIC and MBC results of 100% date ethanolic extract and CDN

| Test | 100% date ethanolic extract concentration (mg/mL) | CDN (mg/mL) | *P* value |
|---|---|---|---|
| **MIC** | 91.5 | 4.5 | < 0.05 |
| **MBC** | 183 | 18 | < 0.05 |

## Conclusions

Cystic fibrosis is a disorder that causes severe damage to the respiratory system. The disease causes excessive production of mucus, sweat, and digestive juices, resulting in the production of sticky and thick secretions that block passageways, ducts, and tubes, especially in the lungs. Long-term concerns pertinent to cystic fibrosis include difficulty

breathing, coughing up mucus, and the buildup of mucus in the lungs, which facilitates bacterial growth and causes infections, particularly with *Pseudomonas aeruginosa*. Therefore, this research developed nanoparticulate DPI formulations containing dried date fruit extract as a potential candidate for the management of cystic fibrosis. There are many effective compounds in date fruit that demonstrate an antibacterial effect. Chitosan-based nanoparticles were prepared and assessed for their aerodynamic performance. Results revealed that low-chitosan nanoparticles (0.05% w/v) had the highest EE of 56% and delivered the highest FPF-ND (42.63%). The CDN was 3 × more effective than the extract, against *P. aeruginosa* biofilm formation. On the other hand, NGI studies revealed that the appropriate amount of prepared CDN that produced the inhibition effect on biofilms could be successfully delivered to the lungs and act locally at the target site where bronchial bacterial biofilms form. This is the first time XRD and *P. aeruginosa* biofilm inhibition data have been reported for date fruit extract nanoparticles. The result of this work suggests that date fruit extract can be employed as an adjuvant for the management of chronic conditions such as CF via targeted pulmonary delivery with reduced systemic exposure. Further applications of this work will involve in vivo and then clinical investigations to evaluate its suitability in clinical practice for the management of CF and other respiratory conditions.

**Supplementary Information** The online version contains supplementary material available at https://doi.org/10.1007/s12247-023-09752-3.

**Acknowledgements** The authors would like to acknowledge Kingston University, Isra University, Najran University, and Aston University for their support towards Eman Dahmash, Nisreen Dahshan, Hamad Alyami, and Affiong Iyrie's work in this research, respectively.

**Author Contribution** E.Z.D: conceptualization, formal analysis, methodology, project administration, supervision, writing original draft, review, and editing. H.A.R: data curation, formal analysis, investigation, methodology, and writing—original draft preparation. N.D: formal analysis, methodology, supervision, and writing—review and editing. H.A: formal analysis, investigation, and writing—review and editing. A.I: formal analysis and writing—review and editing.

**Funding** This research project was funded by Isra University (Jordan) for Hadeel Aburass towards her MSc studies.

**Data Availability Statement** All data generated or analyzed during this study are included in this article.

## Declarations

**Conflict of Interest** The authors declare no competing interests.



## References

1. Rohlfs EM, Zhou Z, Heim RA, Nagan N, Rosenblum LS, Flynn K, et al. Cystic fibrosis carrier testing in an ethnically diverse US population. Clin Chem. 2011;57(6):841–8.
2. Sockrider MM, Ferkol TW. Twenty facts about cystic fibrosis. Am J Respir Crit Care Med. 2017;196(12):P23.
3. Wright CC, Vera YY. Chapter 29 - Cystic fibrosis, in DiPiro J.T., Talbert R.L., Yee G.C., Matzke G.R., Wells B.G., and Posey L. (Eds.), Pharmacotherapy: A Pathophysiologic Approach, 10e. McGraw Hill, New York. 2017;417.
4. Rasamiravaka T, Labtani Q, Duez P, El Jaziri M. The formation of biofilms by Pseudomonas aeruginosa: a review of the natural and synthetic compounds interfering with control mechanisms. Biomed Res Int. 2015;2015.
5. de Boer AH, Hagedoorn P, Hoppentocht M, Buttini F, Grasmeijer F, Frijlink HW. Dry powder inhalation: past, present and future. Expert Opin Drug Deliv. 2017;14(4):499–512.
6. Melander RJ, Melander C. The challenge of overcoming antibiotic resistance: an adjuvant approach? ACS Infect Dis. 2017;3(8):559–63.
7. Wright GD. Antibiotic adjuvants: rescuing antibiotics from resistance. Trends Microbiol. 2016;24(11):862–71.
8. Al-Shahib W, Marshall RJ. The fruit of the date palm: its possible use as the best food for the future? Int J Food Sci Nutr. 2003;54(4):247–59.
9. Mansouri A, Embarek G, Kokkalou E, Kefalas P. Phenolic profile and antioxidant activity of the Algerian ripe date palm fruit (Phoenix dactylifera). Food Chem. 2005;89(3):411–20.
10. Gu L, Kelm MA, Hammerstone JF, Beecher G, Holden J, Haytowitz D, et al. Screening of foods containing proanthocyanidins and their structural characterization using LC-MS/MS and thiolytic degradation. J Agric Food Chem. 2003;51(25):7513–21.
11. Barakat AZ, Hamed AR, Bassuiny RI, Abdel-Aty AM, Mohamed SA. Date palm and saw palmetto seeds functional properties: antioxidant, anti-inflammatory and antimicrobial activities. J Food Meas Charact. 2020;14:1064–72.
12. AlFaris NA, AlTamimi JZ, AlGhamdi FA, Albaridi NA, Alzaheb RA, Aljabryn DH, et al. Total phenolic content in ripe date fruits (Phoenix dactylifera L.): a systematic review and meta-analysis. Saudi J Biol Sci. 2021;28(6):3566–77.
13. Ishurd O, Sun C, Xiao P, Ashour A, Pan Y. A neutral β-d-glucan from dates of the date palm. Phoenix dactylifera L Carbohydr Res. 2002;337(14):1325–8.
14. Badawi JE. Nano particle formulation of Phoenix dactylifera L.(Ajwah and Black date) seed and peel and investigating their antioxidant and antibacterial properties. School of Sciences and Engineering - American University in Cairo; PhD diss., AUC Knowledge Fountain 2018.
15. Zhang C-R, Aldosari SA, Vidyasagar PSPV, Nair KM, Nair MG. Antioxidant and anti-inflammatory assays confirm bioactive compounds in Ajwa date fruit. J Agric Food Chem. 2013;61(24):5834–40.
16. Bahri S, Abdennabi R, Ali R Ben, Mlika M, Gharsallah N, Ayed K, et al. The efficacy of Phoenix dactylifera L. sap for the treatment of lung injury in a murine model of pulmonary fibrosis. Eur Respiratory Soc. 2018. 52: Suppl. 62, PA3718

17. Bahri S, Abdennabi R, Mlika M, Neji G, Jameleddine S, Ali R Ben. Effect of Phoenix dactylifera L. sap against bleomycin-induced pulmonary fibrosis and oxidative stress in rats: phytochemical and therapeutic assessment. Nutr Cancer. 2019;71(5):781–791.
18. USP-35. Aerosols, nasal sprays, metered-dose inhalers, and dry powder inhalers United States Pharamcopeia, The National Formulary. 35th ed. 2012. 232–253. p.
19. Khaled Z, Dahmash EZ, Koner J, Al Ani R, Alyami H, Naser AY. Assessment of vaping devices as an alternative respiratory drug delivery system. Drug Dev Ind Pharm. 2022;1–11.
20. Kirchner S, Fothergill JL, Wright EA, James CE, Mowat E, Winstanley C. Use of artificial sputum medium to test antibiotic efficacy against Pseudomonas aeruginosa in conditions more relevant to the cystic fibrosis lung. JoVE J Vis Exp. 2012;(64):e3857.
21. Al-Tarawneh SF, Dahmash EZ, Alyami H, Abu-Doleh SM, Al-Ali S, Iyire A, et al. Mechanistic modelling of targeted pulmonary delivery of dactinomycin iron oxide-loaded nanoparticles for lung cancer therapy. Pharm Dev Technol. 2022;0(0):1–12. Available from: https://doi.org/10.1080/10837450.2022.2152047.
22. Qiao C, Ma X, Wang X, Liu L. Structure and properties of chitosan films: effect of the type of solvent acid. Lwt. 2021;135:109984.
23. Pavoni JMF, Luchese CL, Tessaro IC. Impact of acid type for chitosan dissolution on the characteristics and biodegradability of cornstarch/chitosan based films. Int J Biol Macromol. 2019;138:693–703.
24. Velásquez-Cock J, Ramírez E, Betancourt S, Putaux J-L, Osorio M, Castro C, et al. Influence of the acid type in the production of chitosan films reinforced with bacterial nanocellulose. Int J Biol Macromol. 2014;69:208–13.
25. Wolkers WF, Oliver AE, Tablin F, Crowe JH. A Fourier-transform infrared spectroscopy study of sugar glasses. Carbohydr Res. 2004;339(6):1077–85.
26. Song C, Yu H, Zhang M, Yang Y, Zhang G. Physicochemical properties and antioxidant activity of chitosan from the blowfly Chrysomya megacephala larvae. Int J Biol Macromol. 2013;60:347–54.
27. Vino AB, Ramasamy P, Shanmugam V, Shanmugam A. Extraction, characterization and in vitro antioxidative potential of chitosan and sulfated chitosan from Cuttlebone of Sepia aculeata Orbigny, 1848. Asian Pac J Trop Biomed. 2012;2(1):S334–41.
28. Queiroz MF, Teodosio Melo KR, Sabry DA, Sassaki GL, Rocha HAO. Does the use of chitosan contribute to oxalate kidney stone formation? Mar Drugs. 2014;13(1):141–58.
29. George N, Andersson AAM, Andersson R, Kamal-Eldin A. Lignin is the main determinant of total dietary fiber differences between date fruit (Phoenix dactylifera L.) varieties. NFS J. 2020;21:16–21.
30. Farhadi S, Ajerloo B, Mohammadi A. Green biosynthesis of spherical silver nanoparticles by using date palm (Phoenix dactylifera) fruit extract and study of their antibacterial and catalytic activities. Acta Chim Slov. 2017;64(1):129–43.
31. Kumar S, Koh J. Physiochemical, optical and biological activity of chitosan-chromone derivative for biomedical applications. Int J Mol Sci. 2012;13(5):6102–16.
32. Govindan S, Nivethaa EAK, Saravanan R, Narayanan V, Stephen A. Synthesis and characterization of chitosan–silver nanocomposite. Appl Nanosci [Internet]. 2012;2(3):299–303. Available from: https://doi.org/10.1007/s13204-012-0109-5.
33. Tang ESK, Huang M, Lim LY. Ultrasonication of chitosan and chitosan nanoparticles. Int J Pharm. 2003;265(1–2):103–14.
34. Yahya MZA, Harun MK, Ali AMM, Mohammat MF, Hanafiah M, Ibrahim SC, et al. XRD and surface morphology studies on chitosan-based film electrolytes. J Appl Sci. 2006;6(15):3150–4.
35. Alyami HS, Ali DK, Jarrar Q, Jaradat A, Aburass H, Mohammed AA, et al. Taste masking of promethazine hydrochloride using l-arginine polyamide-based nanocapsules. Molecules [Internet]. 2023;28(2). Available from: https://www.mdpi.com/1420-3049/28/2/748.
36. Omar Zaki SS, Ibrahim MN, Katas H. Particle size affects concentration-dependent cytotoxicity of chitosan nanoparticles towards mouse hematopoietic stem cells. J Nanotechnol. 2015;2015.
37. Sreekumar S, Goycoolea FM, Moerschbacher BM, Rivera-Rodriguez GR. Parameters influencing the size of chitosan-TPP nano-and microparticles. Sci Rep. 2018;8(1):1–11.
38. Kou SG, Peters L, Mucalo M. Chitosan: a review of molecular structure, bioactivities and interactions with the human body and micro-organisms. Carbohydr Polym. 2022;119132.
39. Lazaridou M, Christodoulou E, Nerantzaki M, Kostoglou M, Lambropoulou DA, Katsarou A, et al. Formulation and in-vitro characterization of chitosan-nanoparticles loaded with the iron chelator deferoxamine mesylate (DFO). Pharmaceutics. 2020;12(3):238.
40. Zhang H, Wu S, Tao Y, Zang L, Su Z. Preparation and characterization of water-soluble chitosan nanoparticles as protein delivery system. J Nanomater. 2010;2010.
41. Wu Y, Yang W, Wang C, Hu J, Fu S. Chitosan nanoparticles as a novel delivery system for ammonium glycyrrhizinate. Int J Pharm. 2005;295(1–2):235–45.
42. Vandenberg GW, Drolet C, Scott SL, De la Noüe J. Factors affecting protein release from alginate–chitosan coacervate microcapsules during production and gastric/intestinal simulation. J Control Release. 2001;77(3):297–307.
43. Buttini F, Brambilla G, Copelli D, Sisti V, Balducci AG, Bettini R, et al. Effect of flow rate on in vitro aerodynamic performance of NEXThaler® in comparison with Diskus® and Turbohaler® dry powder inhalers. J Aerosol Med Pulm Drug Deliv. 2015;29(2):167–78.
44. Dahmash EZ, Ali DK, Alyami HS, Abdulkarim H, Alyami MH, Aodah AH. Novel thymoquinone nanoparticles using poly(ester amide) based on L-arginine-targeting pulmonary drug delivery. Polymers (Basel). 2022;14(6).
45. Dahmash EZ, Ali DK, Alyami HS, Abdulkarim H, Alyami MH, Aodah AH. Novel thymoquinone nanoparticles using poly (ester amide) based on L-arginine-targeting pulmonary drug delivery. Polymers. 2022;14(6):1082.
46. Alyami MH, Dahmash EZ, Ali DK, Alyami HS, AbdulKarim H, Alsudir SA. Novel fluticasone propionate and salmeterol fixed-dose combination nano-encapsulated particles using polyamide based on L-lysine. Pharmaceuticals. 2022;15(3):321.
47. Demoly P, Hagedoorn P, De Boer AH, Frijlink HW. The clinical relevance of dry powder inhaler performance for drug delivery. Vol. 108, Respiratory Medicine. Elsevier Ltd; 2014. 1195–1203 p.
48. Mangal S, Gao W, Li T, Zhou Q (Tony). Pulmonary delivery of nanoparticle chemotherapy for the treatment of lung cancers: challenges and opportunities. Acta Pharmacol Sin. 2017;38(6):782–97.
49. Gharse S, Fiegel J. Large porous hollow particles: lightweight champions of pulmonary drug delivery. Curr Pharm Des. 2016;22(17):2463–9.
50. Ali DK, Al-Ali SH, Dahmash EZ, Edris G, Alyami HS. Reduction and pH dualresponsive biobased poly(disulfide-amide) nanoparticles using cystine amino acid for targeting release of doxorubicin anticancer drug. J Polym Environ. 2022; Available from: https://doi.org/10.1007/s10924-022-02552-9.
51. El-Far AH, Shaheen HM, Abdel-Daim MM, Al-Jaouni SK, Mousa SA. Date palm (Phoenix dactylifera): protection and remedy food. Curr Trends Nutraceuticals. 2016;1:2.
52. Selim S, Alfy SE, Al-Ruwaili M, Abdo A, Jaouni SA. Susceptibility of imipenem-resistant Pseudomonas aeruginosa to flavonoid glycosides of date palm (Phoenix dactylifera L.) tamar growing in Al Madinah, Saudi Arabia. African J Biotechnol. 2012;11(2):416–22.

53. Al-Alawi RA, Al-Mashiqri JH, Al-Nadabi JSM, Al-Shihi BI, Baqi Y. Date palm tree (Phoenix dactylifera L.): natural products and therapeutic options. Front Plant Sci. 2017;8:845.
54. Al Jaouni SK, Hussein A, Alghamdi N, Qari M, El Hossary D, Almuhayawi MS, et al. Effects of Phoenix dactylifera Ajwa on infection, hospitalization, and survival among pediatric cancer patients in a university hospital: a nonrandomized controlled trial. Integr Cancer Ther. 2019;18:1534735419828834.
55. Al-Daihan S, Bhat RS. Antibacterial activities of extracts of leaf, fruit, seed and bark of Phoenix dactylifera. African J Biotechnol. 2012;11(42):10021–5.
56. Chassagne F, Samarakoon T, Porras G, Lyles JT, Dettweiler M, Marquez L, et al. A systematic review of plants with antibacterial activities: a taxonomic and phylogenetic perspective. Front Pharmacol. 2021;11:2069.
57. Hussain MI, Semreen MH, Shanableh A, Khattak MNK, Saadoun I, Ahmady IM, et al. Phenolic composition and antimicrobial activity of different Emirati date (Phoenix dactylifera L.) pits: a comparative study. Plants. 2019;8(11):497.